JOC The Journal of Organic Chemistry

pubs.acs.org/joc Article

Fluoro, Trifluoromethyl, and Trifluoroacetyl Substituent Effects on Cycloaddition Reactivities: Computations and Analysis

Ruirui Su, Kaili Xie, Yong Liang, K. N. Houk, and Fang Liu*

Cite This: *J. Org. Chem.* 2023, 88, 893−900 Read Online

ACCESS | Metrics & More | Article Recommendations | Supporting Information

ABSTRACT: The importance of fluoro and trifluoromethyl substituents in drug effectiveness prompted the computational exploration of fluorine-containing substituents in valuable synthetic cycloadditions. Diels−Alder or 1,3-dipolar cycloaddition reactions of typical reactants, cyclopentadiene, *N*-phenyldiazoacetamide, tetrazine, and *N*-phenylsydnone involving fluorine-containing substituents (F, CF_3, and $COCF_3$) were studied with M06-2X density functional theory. Inductive and conjugative effects influence normal and inverse electron-demand reactions differently. These results provide a guide to the design and use of cycloadditions for the introduction of fluoro and trifluoromethyl substituents in synthetic processes.

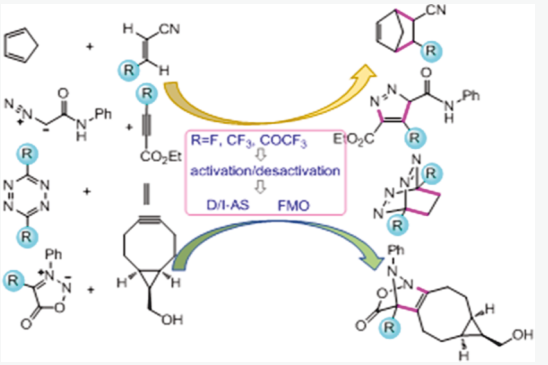

INTRODUCTION

Fluorine-containing substituents often have significant effects on biological and chemical properties of a substrate. About 20% of prescribed and 30% of blockbuster drugs contain fluorine.[1] The insecticide *Teflubenzuron*,[2] *Celecoxib* that treats arthritis,[3] and the antibiotic *Jadomycin N-trifluoroacetyl-L-lysine* (Scheme 1)[4] are prominent examples of these. Fluorine-functionalized materials have been applied in medical and agrochemical practice as well, and there are applications in optical and electronic technologies.[5]

While fluoro substitution may primarily influence physical properties and binding affinities for pharmaceuticals, studies on fluorine-containing substituents show that they have significant electronic effects on cycloaddition reactivities. In 2014, we studied the substituent effects on inverse electron-demand Diels−Alder reactions of 1,2,4,5-tetrazine.[6] Trifluoromethyl destabilizes tetrazines, which leads to smaller distortion energies in the Diels−Alder transition states and therefore smaller activation barriers (Scheme 2a). In 2016, the Raines group studied the 1,3-dipolar cycloaddition of diazomethane derivatives with substituted alkynes and showed that a trifluoromethylalkyne reacts 100 times faster than its ester counterpart.[7] This was attributed to favorable noncovalent interactions (Scheme 2b). In 2016, Taran and co-workers reported ultrafast click chemistry of fluorosydnone, which reacts rapidly and selectively with bicyclo[6.1.0]nonyne (BCN) (Scheme 2c).[8] We and Murphy and co-workers studied the origins of halogen effects in the bioorthogonal cycloadditions of sydnones and discovered that fluorine substitution increases the reactivity of sydnone mainly by lowering its distortion energy.[9] In 2019, Blanchard, Houk, and Liu reported a general strategy for the synthesis of 7-aza-indazoles from 2-hydrazonylpyrimidines via intramolecular Diels−Alder reactions.[10] Computations showed that the activation of the pyrimidine is due to the pre-distortion introduced by trifluoroacetylation (Scheme 2d).

These experimental and computational observations show that fluorine-containing substituents may change cycloaddition reactivities through a variety of mechanisms, by influencing the conformations, distortion energies of reactants, or interaction energies between the reactants. We now present a systematic study of representative cycloadditions, the Diels−Alder reaction of cyclopentadiene with acrylonitrile, the 1,3-dipolar cycloaddition of diazoacetamide with ethyl propiolate, the inverse electron-demand Diels−Alder reaction of tetrazine with ethylene, and the 1,3-dipolar cycloaddition of *N*-phenylsydnone with BCN. We analyze how fluoride, trifluoromethyl, and trifluoroacetyl substituents affect cycloaddition reactivities and provide general guidelines for future developments.

Computational Methods. All calculations were performed with Gaussian 09.[11] Geometry optimizations of the minima and transition states were carried out at the M06-2X level of theory with the 6-31+G(d) basis set and the CPCM model for solvents.[12,13] Vibrational frequencies were computed at the same level to verify that optimized structures are energy minima or transition structures and to evaluate zero-point vibrational

Received: September 20, 2022
Published: December 30, 2022

Scheme 1. Some Bioactive Molecules Containing Fluorine

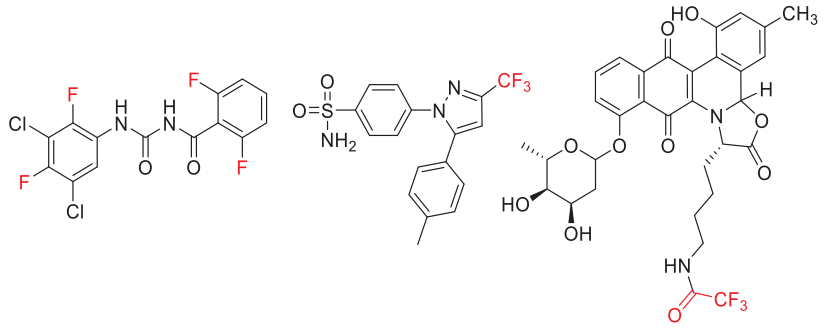

Scheme 2. Previous Experimental/Computational Studies of Fluorine-Containing Substituent Effects on Diels–Alder and 1,3-Dipolar Cycloadditions[a]

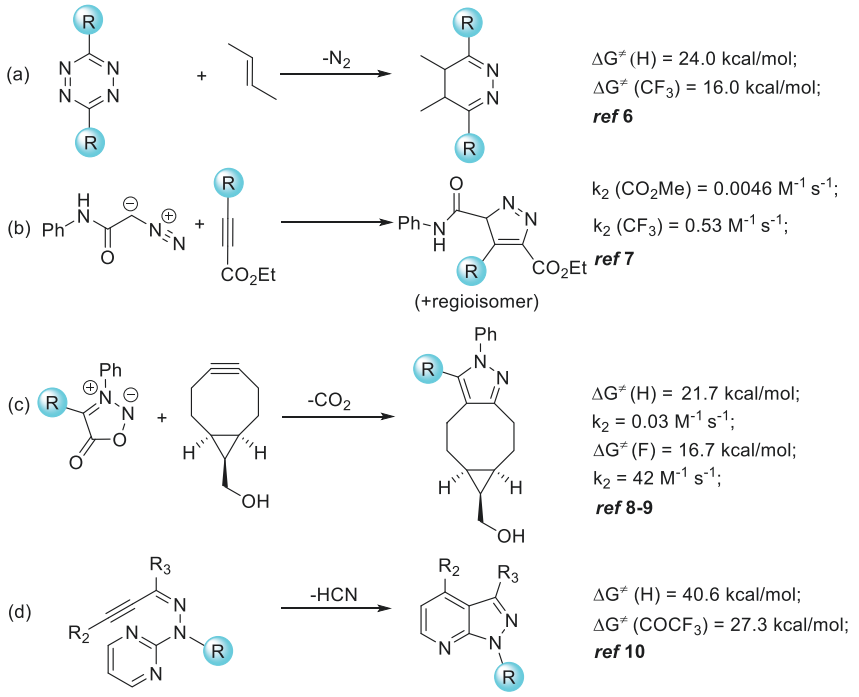

[a]In each case, activation barriers and/or second-order rate constants are compared for H- and the corresponding F-containing group, except for Scheme 2b, where CO_2Me and CF_3 are compared.

energies and thermal corrections at 298 K. Previous studies showed that this method gives relatively accurate energetics for cycloaddition reactions.[14] Energies were evaluated on optimized structures using the same functional with a larger basis set 6-311+G(d,p) and the same solvent model. Frontier molecular orbitals (FMOs) and their energies were computed at the HF/6-311+G(d,p) level on optimized geometries.[15] Distortion/interaction analysis was done at the M06-2X/6-311+G(d,p) level. Optimized structures are illustrated using CYLview.[16] Computational details are provided in the Supporting Information (S10).

Distortion/interaction-activation strain (D/I-AS) analyses on the transition states were carried out to understand the activation or deactivation effects of fluorine-containing substituents.[17−19] In D/I-AS analysis, the transition state structure is separated into two fragments (distorted reactants), followed by single-point energy calculations on each fragment. The energy differences between the distorted fragments and the corresponding separate reactant structures are defined as the distortion energies or activation strains. The difference between the activation energy and the total distortion energy is the interaction energy.

■ RESULTS AND DISCUSSION

Figure 1 summarizes the activation free energies of all 16 reactions studied here (cyclopentadiene with acrylonitrile, diazoacetamide with ethyl propiolate, tetrazine with ethylene, and *N*-phenylsydnone with cyclooctyne, with F, CF_3, and $COCF_3$ substituents). The substituents were attached to the expected electrophilic species in each series as specified by R in Figure 1.

The majority of the cycloaddition reactions follow concerted mechanisms. The reactions of diazoacetamide with fluoro- and trifluoroacetyl-ethyl propiolate have concerted and stepwise barriers (see Supporting Information, Figures S3 and S4), but we used the concerted TSs in our analyses. The following

https://doi.org/10.1021/acs.joc.2c02264
J. Org. Chem. 2023, 88, 893−900

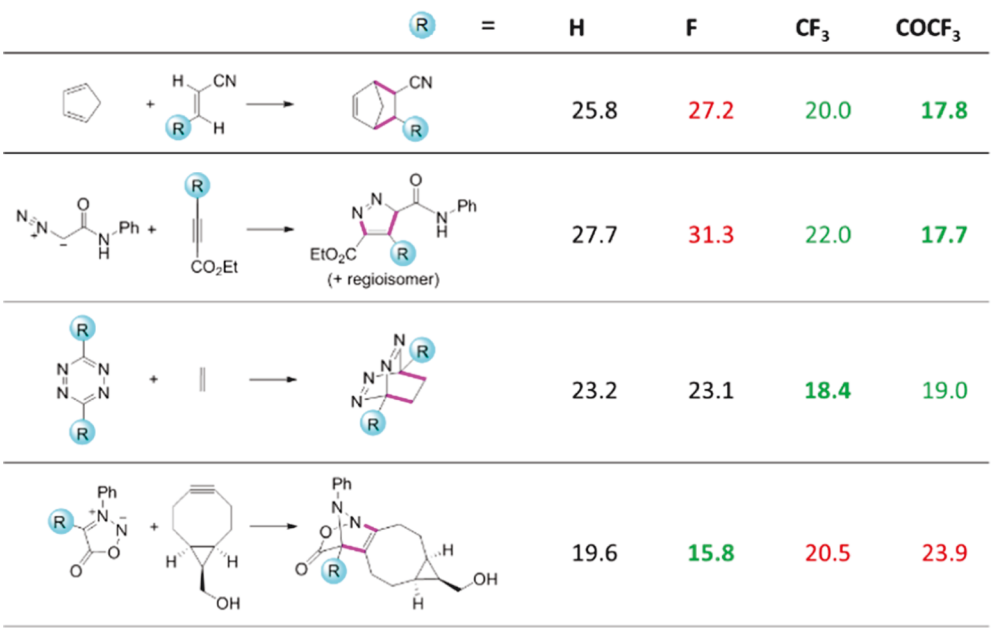

Figure 1. Activation free energies for the cycloaddition reaction of cyclopentadiene, diazoacetamide, tetrazine, and *N*-phenylsydnone (activation-free energies are shown in kcal/mol).

sections include detailed analyses of the reactivity trends, but certain observations can be made at the outset.

The reaction of cyclopentadiene with acrylonitrile is a classic "normal electron-demand" Diels–Alder cycloaddition. Electron-withdrawing CF_3 and $COCF_3$ lower the barriers by 5.8 and 8.0 kcal/mol, respectively, consistent with the electron-withdrawing nature of the substituents ($\sigma_{R\_}CF_3$ = 0.16 and $\sigma_{R\_}COCF_3$ = 0.26).[20] F is inductively electron-withdrawing ($\sigma_{R\_}$ F = −0.32),[21] but due to its resonance electron-donating nature, the reaction barrier is increased by 1.4 kcal/mol.

The diazoacetamide reaction also involves an electron-rich 1,3-dipole and electron-deficient dipolarophiles, and the behavior of CF_3 and $COCF_3$ is similar to that in the previous Diels–Alder reactions. Again, fluorine deactivates ethyl propiolate, and this is discussed in detail later.

The tetrazine cycloaddition with ethylene is an "inverse-electron demand" Diels–Alder reaction. Electron-withdrawing CF_3 and $COCF_3$ lower the barrier by 4.8 and 4.2 kcal/mol, respectively, while F has little effect on the cycloaddition reactivity of tetrazine.

In the cycloaddition of *N*-phenylsydnone with BCN, fluorine has an extraordinary accelerating effect,[9] while electron-withdrawing CF_3 and $COCF_3$ deactivate *N*-phenylsydnone by increasing the barriers by 0.9 and 4.3 kcal/mol, respectively.

Figure 2a shows the D/I-AS analysis of the transition state structures of cyclopentadiene cycloaddition with acrylonitrile. Both *endo*- and *exo*-cycloadditions were studied (Figure S1), but only the favored *exo*-cyano pathways are shown here. The TS structures are all asynchronous. $COCF_3$-acrylonitrile has an earlier transition state and a longer forming C–C bond distance than other substituent groups (F, CF_3) (Figure S7).

The change in cyclopentadiene distortion is small across the series (blue arrows, 13.6–14.7 kcal/mol). Dienophile distortion varies more (green arrows, 8.2–12.0 kcal/mol), but the change in interaction energies is most significant (red arrows, −11.8 to −22.9 kcal/mol). For the fluoro substitution, the greater distortion energy, lead to the alkene causes a slight increase in barrier, even though the interaction energy increases. For CF_3 and $COCF_3$, large increases in interaction energy lower the overall free energy barriers by 5.8 and 8.0 kcal/mol, respectively.

To better understand that the interaction energies are significant to lower the free energy barriers, an energy decomposition analysis (EDA) was performed by the cycloaddition of cyclopentadiene with acrylonitrile (Figure 2b). EDA was carried out using the ADF.2018.106 program at the M06-2X/6-311+G(d,p) level of geometries optimized at Gaussian 09.[22] An EDA involves the decomposition of ΔE_{int} into electrostatic (ΔE_{elstat}), Pauli repulsive (ΔE_{Pauli}), dispersion (ΔE_{disp}), polarization energy (ΔE_{pol}), and charge transfer (ΔE_{ct}), as shown in eq 1. The contributions of polarization energy and dispersion are less significant; the electrostatic and charge transfer are systematically more favorable for the cycloaddition of cyclopentadiene with F-containing acrylonitrile, accompanied by more positive Pauli repulsions though. An overall effect is achieved with electrostatics and charge transfer overcoming the Pauli repulsion, which gives rise to a net stabilizing interaction.

$$E_{int} = E_{elec} + E_{ct} + E_{disp} + E_{pol} + E_{pau} \quad (1)$$

The reaction of cyclopentadiene with acrylonitrile involves significant orbital interaction between the HOMO of cyclopentadiene and the LUMO of acrylonitrile. Figure 3 shows the LUMOs of acrylonitrile and the substituted acrylonitriles. There is a correlation between the LUMO energies and interaction energies/activation barriers.[23] The lower the LUMO energy, the greater the interaction energy.

Figure 4 shows the transition structures for 1,3-dipolar cycloaddition of the relatively electron-rich *N*-phenyldiazoacetamide with ethyl propiolates, along with the D/I-AS analysis on each. Both stepwise and concerted pathways were studied for *syn*- and *anti*-cycloadditions (Figures S2–S4), and the TSs of the concerted pathways are shown here. The pattern of reactivity here is very much like that of the cyclopentadiene/acrylonitrile cycloaddition, although the energy changes are slightly different. Fluoro once again increases distortion energies, now for both dipole and dipolarophiles, and the interaction energy also

https://doi.org/10.1021/acs.joc.2c02264
J. Org. Chem. 2023, 88, 893–900

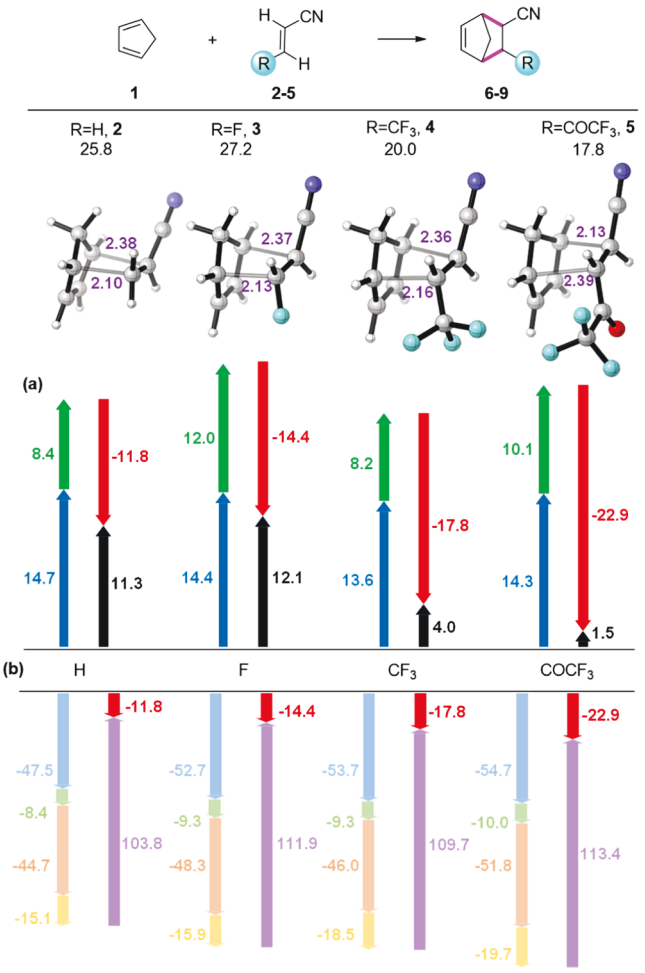

Figure 2. Distortion/interaction analysis on the transition state structures of cyclopentadiene cycloaddition with acrylonitrile (forming bond lengths are shown in Angstroms and activation free energy in kcal/mol). The blue distortion arrow is for cyclopentadiene; green stands for dienophile distortion energy; red stands for interaction energy; black stands for activation electronic energy; baby blue stands for electrostatics; baby green stands for polarization energy; golden stands for charge transfer; yellow stands for dispersion; purple stands for Pauli repulsion.

increases. The net result is a slower reaction and an early transition state with a reversal of regioselectivity (Figure S8). CF_3 once again increases reactivity through a larger interaction energy, and the original regioselectivity is restored, uniting the diazo nucleophile carbon β to ester rather than the CF_3 terminus. The $COCF_3$ group increases the reactivity most, with a free energy barrier of 10 kcal/mol lower (k_2 at RT 107 larger!). The lower interaction and dipole distortion energy is due to the considerably more asynchronous and earlier transition state for this reaction.

Figure 5 shows the FMOs of 1,3-dipole and various substituted ethyl propiolates with coefficients at reacting sites labeled. There is a correlation between the LUMO energies and the interaction energies/activation barriers. Note the large disparity in orbital coefficients on ethyl propiolate with F and $COCF_3$ substituents, in which the ester dominates over F and $COCF_3$ over the ester, respectively. These lead to very unsymmetrical TSs and even competition for stepwise processes (see Supporting Information). The regioselectivity of reactions of the parent propriolate and the CF_3 and $COCF_3$ derivatives are such that the largest diazo HOMO − 2 coefficient is united with the largest dienophile LUMO coefficient. The consistency is the fluoro-substituted case, where the regioselectivity is the result of interaction of the diazo HOMO − 2 (largest coefficient at the terminal C) with the alkyne LUMO, largest coefficient at the fluoro-substituted terminus; this is stepwise but is most favorable. For better comparison, the fluoro-substituted case of the concerted pathways is shown here.

Tetrazine cycloadditions with simple alkenes are inverse-electron-demand Diels−Alder reactions. D/I-AS analyses were carried out on the transition states (Figure 6). Two substituents were placed on the tetrazine for the computations to maintain symmetry and simplicity.

The distortion energies of ethylene only change subtly (green arrows, 3.7−5.2 kcal/mol), while distortion of tetrazine varies according to substitution (blue arrows, 14.0−18.8 kcal/mol). Consistent with our earlier studies,[6] the resonance electron-donating F increases the activation energy, while the two strong acceptors lower the distortion energy and has an early transition state (Figure S9). There are more significant variations in interaction energies (red arrows, −12.1 to −17.9 kcal/mol) which dictate the order of electron withdrawal and LUMO + 1 energy lowering (Figure 7): H < F < CF_3 < $COCF_3$.

Figure 7 shows the LUMO + 1 (p orbital interacting with ethylene HOMO) of substituted tetrazines. There is a correlation between LUMO + 1 energies and interaction

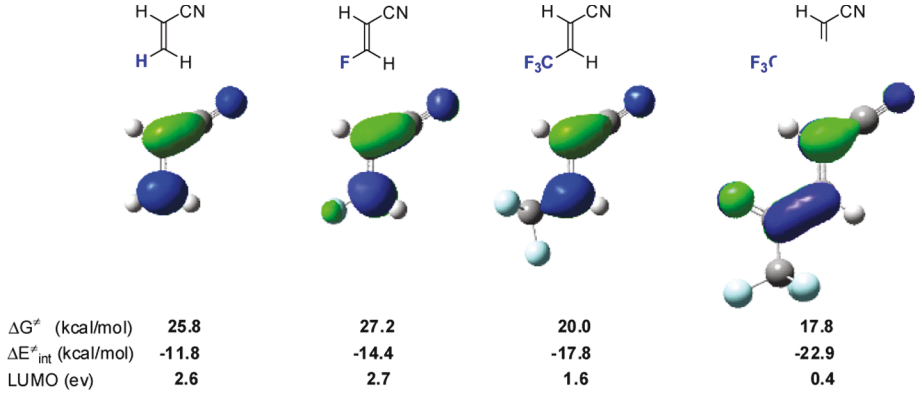

Figure 3. LUMO of acrylonitriles involved in the Diels−Alder reaction with cyclopentadiene. Orbital energies computed at the HF/6-311+G(d,p) level are shown below the orbitals.

https://doi.org/10.1021/acs.joc.2c02264
J. Org. Chem. 2023, 88, 893−900

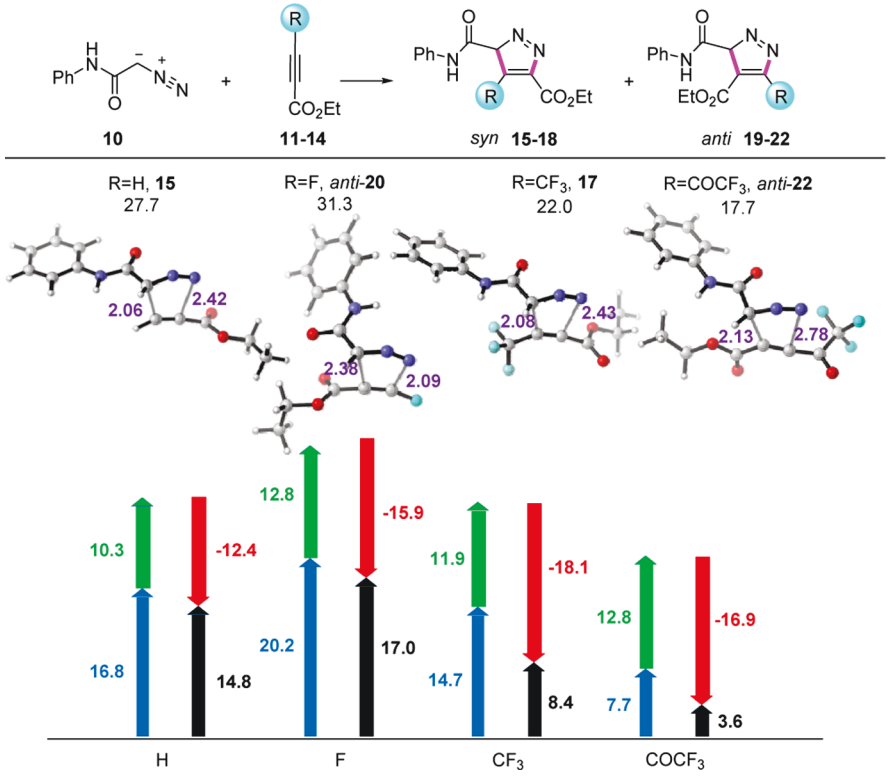

Figure 4. Distortion/interaction analysis on the transition state of *N*-phenyldiazoacetamide cycloaddition with substituted ethyl propiolates (forming bond lengths are shown in Angstroms and activation free energy in kcal/mol). The blue distortion arrow is for *N*-phenyldiazoacetamide; green stands for ethyl propiolate distortion energy; red stands for interaction energy; black stands for activation electronic energy.

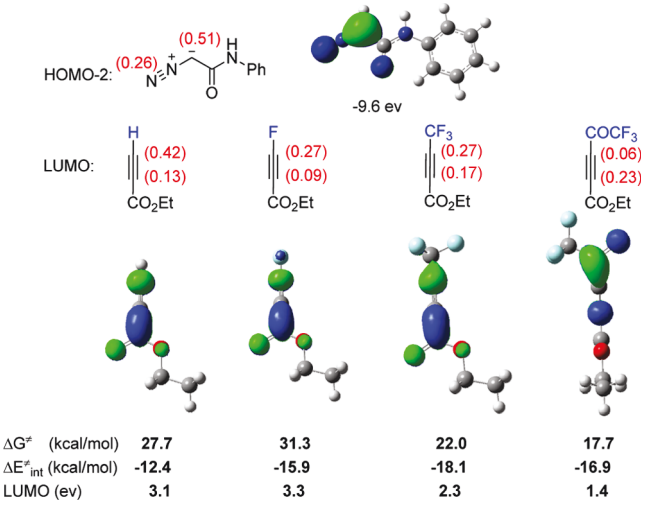

Figure 5. FMOs for the *N*-phenyldiazoacetamide cycloaddition with ethyl propiolates. Numbers in parentheses are sums of squares of the HOMO − 2 or LUMO coefficients at the corresponding atoms.

energies. Because of the role of distortion, the net reactivity order is H = F < CF_3 = $COCF_3$.

Transition structures and D/I-AS analyses on the *N*-phenylsydnone cycloadditions with the especially reactive cyclooctyne are shown in Figure 8.[24] Both *endo*- and *exo*-cycloadditions were studied (Figure S5), but only the favored *exo*-*N*-phenylsydnone pathways are shown here.

5-Fluoro-*N*-phenylsydnone has the longest forming bond distances and therefore early transition state with small distortion, leading to substantial activation, which has been reported in our previous work.[9] On the other hand, CF_3

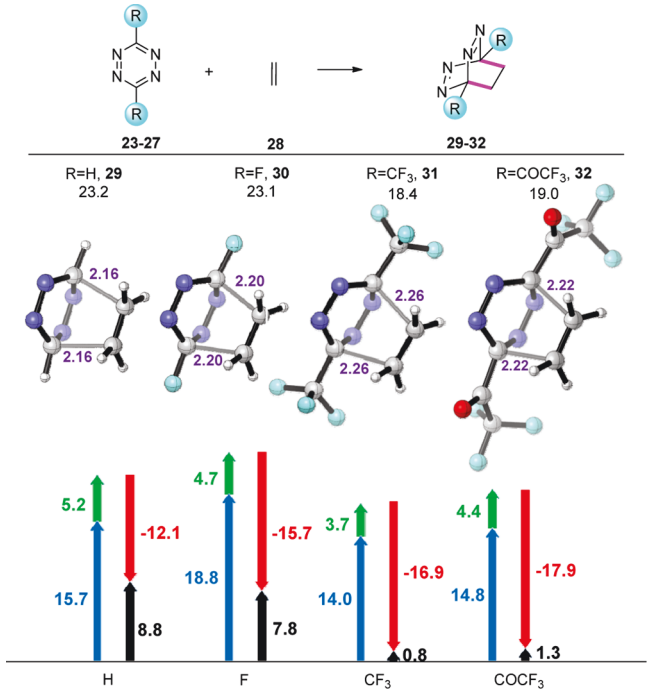

Figure 6. Distortion/interaction analysis on the transition state structures of tetrazine cycloaddition with ethylene (forming bond lengths are shown in Angstroms and activation free energy in kcal/mol). Blue stands for tetrazine distortion, green stands for ethylene distortion energy, red stands for interaction energy, and black stands for activation electronic energy.

https://doi.org/10.1021/acs.joc.2c02264
J. Org. Chem. 2023, 88, 893−900

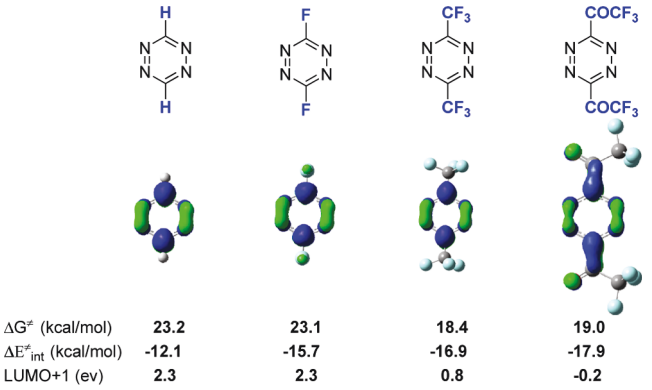

Figure 7. LUMO + 1 of tetrazine involved in the Diels–Alder reaction. Orbital energies are shown below the orbitals.

substitution on *N*-phenylsydnone lowers its reactivity by increased distortion energy. The forming bond distances are almost identical compared to the parent reaction. $COCF_3$ is the most deactivated, and the forming bond distances suggest high asynchronicity but has an early transition state, presumably due to the carbonyl group into a less favorable conformation of *N*-phenylsydnone (Figure S10). To test our hypothesis, we studied other carbonyl substituents ($COCH_3$, CHO). Consistent with our prediction, there is significant deactivation with both cases due to the large distortion energies.

The distortion energies of cyclooctyne are very small across the series (green arrows, 2.4–4.8 kcal/mol), while the distortion energies of *N*-phenylsydnone vary according to the substituent (blue arrows, 12.6–21.2 kcal/mol) and are more significant than the change in interaction energies (red arrows, −13.0 to −16.6 kcal/mol). The resonance electron-donating F lowers the distortion energy; the electron acceptors (CF_3, $COCF_3$, COMe, CHO) make *N*-phenylsydnone harder to distort (Figure 8).

F-substitution activates *N*-phenylsydnone because its resonance electron-donating nature makes sydnone easier to distort. CF_3 is a strong electron acceptor that decreases the reactivity of *N*- phenylsydnone by increasing the distortion energy. $COCF_3$ deactivates *N*-phenylsydnone not only as an electron acceptor but also makes *N*-phenylsydnone harder to distort by the rotation of the carbonyl group into less favorable conformation in the transition state. The change in dihedral angle from the reactant structure to transition state raises the *N*-phenylsydnone distortion energy (Figure S6). CHO and $COCH_3$ have a less significant deactivation effect than $COCF_3$ of *N*-phenylsydnone due to their weaker electron-withdrawing nature. The overall reactivity trend is largely influenced by distortion: F < H < CF_3 < CHO = COMe = $COCF_3$.

The LUMOs of substituted *N*-phenylsydnones are shown in Figure 9. As the LUMO lowers, the interaction energy increases, but that trend is overwhelmed by the distortion energies that ultimately dominate the reactivity trends.

CONCLUSIONS

We studied the fluorine-containing substituent effect on reactivity in cyclopentadiene, *N*-phenyldiazoacetamide, tetrazine, and *N*-phenylsydnone cycloaddition. Trifluoromethyl and trifluoroacetyl have similar activation/deactivation effects in the four types of cycloadditions. They both lower the LUMO of acrylonitrile or LUMO + 1 of tetrazine in DA or inverse-electron

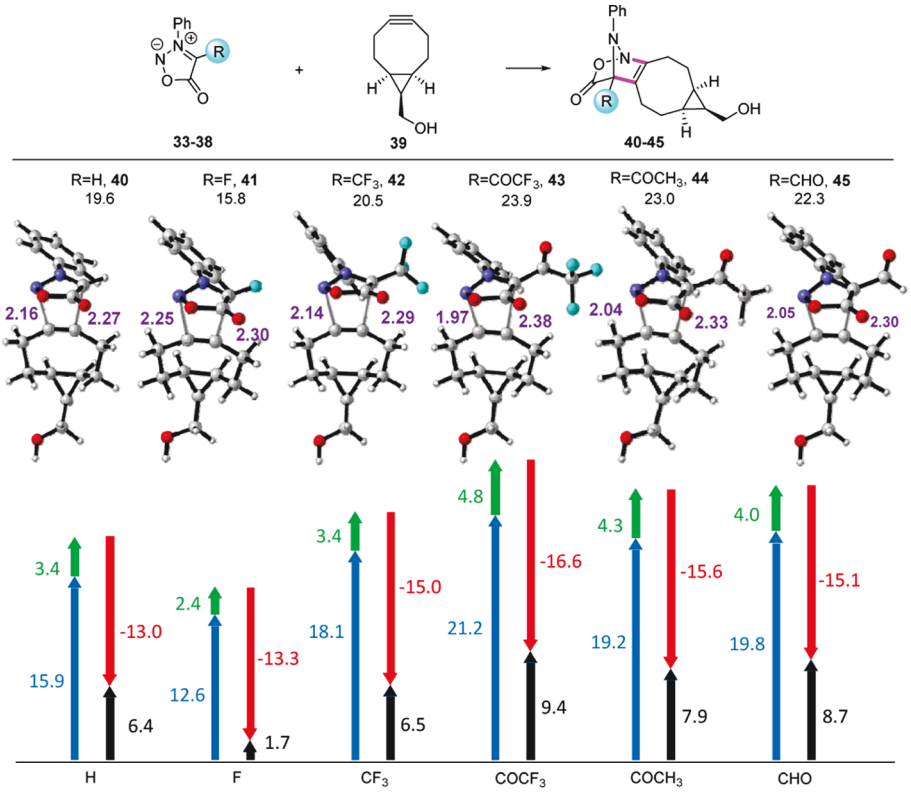

Figure 8. Distortion/interaction model and transition structures of *N*-phenylsydnone cycloaddition with reactive bicyclic cyclooctyne (forming bond lengths are shown in Angstroms and activation free energy in kcal/mol). Blue stands for *N*-phenylsydnone distortion, green stands for cyclooctyne distortion energy, red stands for interaction energy, and black stands for activation electronic energy.

https://doi.org/10.1021/acs.joc.2c02264
J. Org. Chem. 2023, 88, 893–900

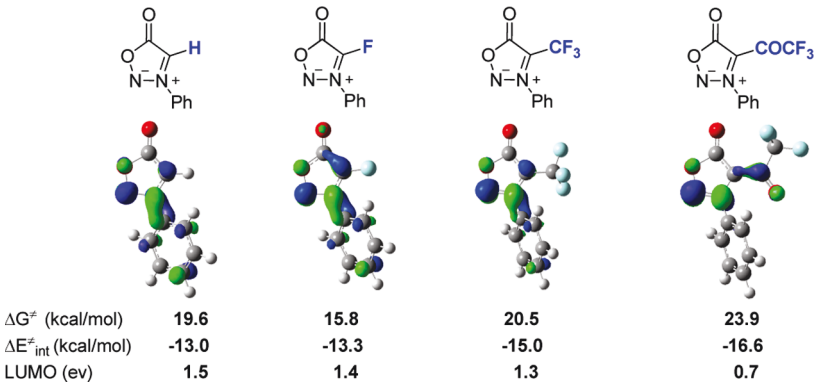

Figure 9. LUMO of *N*-phenylsydnone involved in the Diels–Alder reaction. Orbital energies are shown below the orbitals.

demand DA reactions, and the increase in stabilizing interaction correlates with high reactivities. Fluorine, on the other hand, has a significant activation effect on *N*-phenylsydnone, where distortion is the determining factor. An in-depth understanding of how fluorine-containing substituents affect reactivities provides helpful guide to future development of new reactions.

■ ASSOCIATED CONTENT

Data Availability Statement

data-availability:The data underlying this study are available in the published article and its online Supporting Information

Supporting Information

The Supporting Information is available free of charge at https://pubs.acs.org/doi/10.1021/acs.joc.2c02264.

Computational details including additional results, methods, and cartesian coordinates (PDF)

■ AUTHOR INFORMATION

Corresponding Author

Fang Liu – *College of Sciences, Nanjing Agricultural University, Nanjing 210095, China;* orcid.org/0000-0002-0046-8434; Email: acialiu@njau.edu.cn

Authors

Ruirui Su – *College of Sciences, Nanjing Agricultural University, Nanjing 210095, China*

Kaili Xie – *College of Sciences, Nanjing Agricultural University, Nanjing 210095, China*

Yong Liang – *School of Chemistry and Chemical Engineering, Nanjing University, Nanjing 210023, China;* orcid.org/0000-0001-5026-6710

K. N. Houk – *Department of Chemistry and Biochemistry, University of California, Los Angeles, California 90095, United States;* orcid.org/0000-0002-8387-5261

Complete contact information is available at: https://pubs.acs.org/10.1021/acs.joc.2c02264

Author Contributions

Conception (R.R.S.; K.L.X.; Y.L.; K.N.H.; F.L.); execution and analysis (R.R.S.), and writing manuscript (R.R.S.; K.L.X.; Y.L.; K.N.H.; F.L.).

Notes

The authors declare no competing financial interest.

■ ACKNOWLEDGMENTS

We are grateful for financial support from the Natural Science Foundation of Jiangsu Province, China (BK20190505), the US National Science Foundation grant (CHE-1764328), and the National Nature Science Foundation of China (22077062).

■ REFERENCES

(1) (a) O'Hagan, D. Fluorine in health care: Organofluorine containing blockbuster drugs. *J. Fuorine Chem.* **2010**, *131*, 1071–1081. (b) Hiyama, T.. *Organofluorine Compounds; Chemistry and Applications*; Yamamoto, H., Ed.; Springer: New York, 2000. and references therein.. In (c) Wang, J.; Sánchez-Roselló, M.; Aceña, J. L.; del Pozo, C. del.; Sorochinsky, A. E.; Fustero, S.; Soloshonok, V. A.; Liu, H. L.. Fluorine in Pharmaceutical Industry: Fluorine-Containing Drugs Introduced to the Market in the Last Decade (2001-2011). *Chem. Rev.* **2014**, *114*, 2432–2506. (d) Fujiwara, T.; O'Hagan, D. Successful Fluorine-Containing Herbicide Agrochemicals. *J. Fluorine Chem.* **2014**, *167*, 16–29. (e) Berger, R.; Resnati, G.; Metrangolo, P.; Weber, E.; Hulliger, J. Organic fluorine compounds: a great opportunity for enhanced materials properties. *Chem. Soc. Rev.* **2011**, *40*, 3496–3508.

(2) (a) Khaled, M. B.; El Mokadem, R. K.; Weaver, J. D. Hydrogen bond directed photocatalytic hydrodefluorination: overcoming electronic control. *J. Am. Chem. Soc.* **2017**, *139*, 13092–13101. (b) Selby, T. P.; Bereznak, J. F.; Bisaha, J. J.; Ding, A. X.; Gopalsamuthiram, V.; Hanagan, M. A.; Long, J. K.; Taggi, A. E.; Du Pont de Nemours, E. I.; Company, USA.Substituted azoles as fungicides and their preparation; International Patent WO2009137651A2, 2009. (c) Gregory, V.; Taggi, A. E.; Du Pont de Nemours, E. I.; Company, USA.Preparation of fungicidal imidazole derivatives, their mixtures with other fungicides, and use for controlling plant diseases caused by fungal plant pathogens; International Patent WO2011056463A2, 2011.

(3) Ilardi, E. A.; Vitaku, E.; Njardarson, J. T. Data-mining for sulfur and fluorine: an evaluation of pharmaceuticals to reveal opportunities for drug design and discovery. *J. Med. Chem.* **2014**, *57*, 2832–2842.

(4) Forget, S. M.; Robertson, A. W.; Overy, D. P.; Kerr, R. G.; Jakeman, D. L. Furan and Lactam Jadomycin Biosynthetic Congeners Isolated from Streptomyces venezuelae ISP5230 Cultured with Nε-Trifluoroacetyl-l-lysine. *Nat. Prod.* **2017**, *80*, 1860–1866.

(5) Champagne, P. A.; Desroches, J.; Hamel, J. D.; Vandamme, M.; Paquin, J. F. Monofluorination of organic compounds: 10 years of innovation. *Chem. Rev.* **2015**, *115*, 9073–9174.

(6) Liu, F.; Liang, Y.; Houk, K. N. Theoretical elucidation of the origins of substituent and strain effects on the rates of Diels-Alder reactions of 1,2,4,5-tetrazines. *J. Am. Chem. Soc.* **2014**, *136*, 11483–11493.

(7) Gold, B.; Aronoff, M. R.; Raines, R. T. 1,3-Dipolar Cycloaddition with Diazo Groups: Noncovalent Interactions Overwhelm Strain. *Org. Lett.* **2016**, *18*, 4466–4469.

(8) Liu, H.; Audisio, D.; Plougastel, L.; Decuypere, E.; Buisson, D.-A.; Koniev, O.; Kolodych, S.; Wagner, A.; Elhabiri, M.; Krzyczmonik, A.; Forsback, S.; Solin, O.; Gouverneur, V.; Taran, F. Ultrafast click

chemistry with fluorosydnones. *Angew. Chem., Int. Ed.* **2016**, *55*, 12073−12077.
(9) Tao, H. M.; Liu, F.; Zeng, R. X.; Shao, Z. Z.; Zou, L. F.; Cao, Y.; Murphy, J. M.; Houk, K. N.; Liang, Y. Origins of halogen effects in bioorthogonal sydnone cycloadditions. *Chem. Commun.* **2018**, *54*, 5082−5085.
(10) Le Fouler, V. L.; Chen, Y.; Gandon, V.; Bizet, V.; Salomé, C.; Fessard, T.; Liu, F.; Houk, K. N.; Blanchard, N. Activating Pyrimidines by Pre-distortion for the General Synthesis of 7-Aza-indazoles from 2-Hydrazonylpyrimidines via Intramolecular Diels-Alder Reactions. *J. Am. Chem. Soc.* **2019**, *141*, 15901−15909.
(11) Frisch, M. J.; Trucks, G. W.; Schlegel, H. B.; Scuseria, G. E.; Robb, M. A.; Cheeseman, J. R.; Scalmani, G.; Barone, V.; Mennucci, B.; Petersson, G. A.; Nakatsuji, H.; Caricato, M.; Li, X.; Hratchian, H. P.; Izmaylov, A. F.; Bloino, J.; Zheng, G.; Sonnenberg, J. L.; Hada, M.; Ehara, M.; Toyota, K.; Fukuda, R.; Hasegawa, J.; Ishida, M.; Nakajima, T.; Honda, Y.; Kitao, O.; Nakai, H.; Vreven, T.; Montgomery, J. A.; Peralta, J. E.; Ogliaro, F.; Bearpark, M.; Heyd, J. J.; Brothers, E.; Kudin, K. N.; Staroverov, V. N.; Keith, T.; Kobayashi, R.; Normand, J.; Raghavachari, K.; Rendell, A.; Burant, J. C.; Iyengar, S. S.; Tomasi, J.; Cossi, M.; Rega, N.; Millam, J. M.; Klene, M.; Knox, J. E.; Cross, J. B.; Bakken, V.; Adamo, C.; Jaramillo, J.; Gomperts, R.; Stratmann, R. E.; Yazyev, O.; Austin, A. J.; Cammi, R.; Pomelli, C.; Ochterski, J. W.; Martin, R. L.; Morokuma, K.; Zakrzewski, V. G.; Voth, G. A.; Salvador, P.; Dannenberg, J. J.; Dapprich, S.; Daniels, A. D.; Farkas, O.; Foresman, J. B.; Ortiz, J. V.; Cioslowski, J.; Fox, D. J.*Gaussian 09*, revision D.01; Gaussian Inc.: Wallingford, CT, 2013.
(12) (a) Zhao, Y.; Truhlar, D. G. The M06 suite of density functionals for main group thermochemistry, thermochemical kinetics, noncovalent interactions, excited states, and transition elements: two new functionals and systematic testing of four M06-class functionals and 12 other functionals. *Theor. Chem. Acc.* **2008**, *120*, 215−241. (b) Zhao, Y.; Truhlar, D. G. Density functionals with broad applicability in chemistry. *Acc. Chem. Res.* **2008**, *41*, 157−167. (c) de la Concepcijn, J. G.; Avalos, M.; Cintas, P.; Jiménez, J. L. Computational screening of new orthogonal metal-free dipolar cycloadditions of mesomeric betaines. *Chem.—Eur. J.* **2018**, *24*, 7507−7512.
(13) (a) Barone, V.; Cossi, M. Quantum calculation of molecular energies and energy gradients in solution by a conductor solvent model. *J. Phys. Chem. A* **1998**, *102*, 1995−2001. (b) Cossi, M.; Rega, N.; Scalmani, G.; Barone, V. Energies, structures, and electronic properties of molecules in solution with the C-PCM solvation model. *J. Comput. Chem.* **2003**, *24*, 669−681. (c) Takano, Y.; Houk, K. N. Benchmarking the conductor-like polarizable continuum model (CPCM) for aqueous solvation free energies of neutral and ionic organic molecules. *J. Chem. Theory Comput.* **2005**, *1*, 70−77.
(14) (a) Paton, R. S.; Mackey, J. L.; Kim, W. H.; Lee, J. H.; Danishefsky, S. J.; Houk, K. N. Origins of Stereoselectivity in the trans Diels−Alder Paradigm. *J. Am. Chem. Soc.* **2010**, *132*, 9335−9340. (b) Lan, Y.; Zou, L. F.; Cao, Y.; Houk, K. N. Computational methods to calculate accurate activation and reaction energies of 1,3-dipolar cycloadditions of 24 1,3-dipoles. *J. Phys. Chem. A* **2011**, *115*, 13906−13920.
(15) (a) Politzer, P.; Abu-Awwad, F. A comparative analysis of Hartree-Fock and Kohn-Sham orbital energies. *Theor. Chem. Acc.* **1998**, *99*, 83−87. (b) Kar, T.; Ángyán, J. G.; Sannigrahi, A. B. Comparison of ab Initio Hartree−Fock and Kohn−Sham Orbitals in the Calculation of Atomic Charge, Bond Index, and Valence. *J. Phys. Chem. A* **2000**, *104*, 9953−9963. (c) Zhang, G.; Musgrave, C. B. Comparison of DFT methods for molecular orbital eigenvalue calculations. *J. Phys. Chem. A* **2007**, *111*, 1554−1561.
(16) Legault, C. Y.*CYLview, 1.0b*; Universite de Sherbrooke: Quebee: Montreal, Canada, 2009. http://www.cylview.org.
(17) (a) Ess, D. H.; Houk, K. N. Distortion/interaction energy control of 1,3-dipolar cycloaddition reactivity. *J. Am. Chem. Soc.* **2007**, *129*, 10646−10647. (b) Ess, D. H.; Houk, K. N. Theory of 1,3-dipolar cycloadditions: distortion/interaction and frontier molecular orbital models. *J. Am. Chem. Soc.* **2008**, *130*, 10187−10198.
(18) (a) van Zeist, W. J.; Bickelhaupt, F. M. The activation strain model of chemical reactivity. *Org. Biomol. Chem.* **2010**, *8*, 3118−3127. (b) Fernández, I. Combined activation strain model and energy decomposition analysis methods: a new way to understand pericyclic reactions. *Phys. Chem. Chem. Phys.* **2014**, *16*, 7662−7671.
(19) For examples, see: (a) Fernández, I.; Bickelhaupt, F. M. Alder-ene reaction: aromaticity and activation-strain analysis. *J. Comput. Chem.* **2012**, *33*, 509−516. (b) Fernández, I.; Bickelhaupt, F. M.; Cossío, F. P. Type-I dyotropic reactions: understanding trends in barriers. *Chem.—Eur. J.* **2012**, *18*, 12395−12403. (c) Lopez, S. A.; Houk, K. N. Alkene distortion energies and torsional effects control reactivities, and stereoselectivities of azide cycloadditions to norbornene and substituted norbornenes. *J. Org. Chem.* **2013**, *78*, 1778−1783. (d) Zou, L.; Paton, R. S.; Eschenmoser, A.; Newhouse, T. R.; Baran, P. S.; Houk, K. N. Enhanced reactivity in dioxirane C-H oxidations via strain release: a computational and experimental study. *J. Org. Chem.* **2013**, *78*, 4037−4048. (e) Hong, X.; Liang, Y.; Houk, K. N. Mechanisms and origins of switchable chemoselectivity of Ni-catalyzed C(aryl)-O and C(acyl)-O activation of aryl esters with phosphine ligands. *J. Am. Chem. Soc.* **2014**, *136*, 2017−2025. (f) Fernández, I.; Bickelhaupt, F. M. The activation strain model and molecular orbital theory: understanding and designing chemical reactions. *Chem. Soc. Rev.* **2014**, *43*, 4953−4967. (g) Bickelhaupt, F. M.; Houk, K. N. Analyzing reaction rates with the distortion/interaction-Activation strain model. *Angew. Chem., Int. Ed.* **2017**, *56*, 10070−10086. (h) Vermeeren, P.; Hamlin, T. A.; Bickelhaupt, F. M. Chemical reactivity from an activation strain perspective. *Chem. Commun.* **2021**, *57*, 5880−5896.
(20) Stock, L. M.; Wasielewski, M. R. The Trifluoromethyl Group in Chemistry and Spectroscopy. Carbon-Fluorine Hyperconjugation. *Prog. Phys. Org. Chem.* **2007**, *13*, 253−313.
(21) Ritchie, C. D.; Sager, W. F. An Examination of Structure-Reactivpity Relationships. *Prog. Phys. Org. Chem.* **1964**, *2*, 323−465.
(22) te Velde, G.; Bickelhaupt, F. M.; Baerends, E. J.; Fonseca Guerra, C. F.; van Gisbergen, S. J. A.; Snijders, J. G.; Ziegler, T. Chemistry with ADF. *J. Comput. Chem.* **2001**, *22*, 931−967.
(23) (a) Arpa, E. M.; Aguilar-Galindo, F. A.; Díaz-Tendero, S. D. Unravelling the Mechanism of Non-photoactivated [2+2] Cycloaddition Reactions: Relevance of Orbital Interactions and Zwitterionic Intermediates. *ChemistrySelect* **2017**, *2*, 1089−1093. (b) Shahrestani, N.; Khosravi, H.; Jadidi, K.; Notash, B.; Naderi, S. Organocatalytic synthesis of enantiopure spiro acenaphthyl-pyrrolizidine/pyrrolidines: justifying the regioselectivity based on a distortion/interaction model. *Org. Biomol. Chem.* **2019**, *17*, 7013−7024.
(24) Plougastel, L.; Koniev, O.; Specklin, S.; Decuypere, E.; Créminon, C.; Buisson, D.-A.; Wagner, A.; Kolodych, S.; Taran, F. 4-Halogeno-sydnones for fast strain promoted cycloaddition with bicyclo-[6.1.0]-nonyne. *Chem. Commun.* **2014**, *50*, 9376−9378.

https://doi.org/10.1021/acs.joc.2c02264
J. Org. Chem. 2023, 88, 893−900